Synthesis and Characterization of Ta_2O_5–SiO_2 Mixed Oxides

Garbine Guiu and Paul Grange*
Catalyse et Chimie des Matériaux Divisés, Université Catholique de Louvain,
Place Croix du Sud 2/17, 1348 Louvain-la-Neuve, Belgium

(Received April 28, 1994)

Mixed oxides, especially silica containing multicomponent oxides, have recently found many applications in the production of glasses, ceramics and catalysts. This paper reports for the first time the synthesis of SiO_2–Ta_2O_5 mixed oxide by the sol–gel method. The advantage of the sol–gel method is that a relatively large concentration of tantalum can be incorporated in the mixed oxide structure. Physicochemical characterization shows that tantalum atoms are incorporated into the silica matrix producing Si–O–Ta bonds.

Mixed oxides represent a small, but important, part of the whole family of inorganic compounds. Different methods have been used for their preparation: (i) the mechanical mixture of powder, (ii) coprecipitation, and more recently (iii) via a technique based on the sol–gel process. By following this sol–gel route extremely pure and homogeneous multicomponent oxides can be synthesised at much lower temperatures than with traditional methods.[1]

The sol–gel method have found many applications particularly in the synthesis of glasses, ceramics, and catalytic materials. In the field of catalysis this method has answered, in part, the demand for new high surface area catalysts and the synthesised multicomponent oxides often possess special catalytic properties.[2] The origin of these catalytic properties can be explained by the creation of new types of catalytic sites by the combination of two single oxides.[3,4]

A great number of silica based solid catalysts have already been synthesised by the sol–gel method: SiO_2–Al_2O_3,[5] SiO_2–Nb_2O_5,[6] SiO_2–V_2O_5,[7] SiO_2–TiO_2,[8] SiO_2–ZrO_2, TiO_2–ZrO_2.[9] Several comprehensive reviews have been recently published.[2,10]

This paper describes, in detail, the synthesis of a new family of multicomponent oxides: Ta_2O_5–SiO_2 mixed oxides, with different tantalum silicon molecular ratios. The study of its structural and textural properties are also presented.

Experimental

Preparation of SiO_2–Ta_2O_5. The SiO_2–Ta_2O_5 mixed oxides were prepared using the sol–gel method.[11,12] This novel method allows the synthesis of mixed oxides by the dehydration, at low temperatures, of an amorphous gel formed in a solution. In the sol–gel method, an inorganic polymer is formed, by the way of a condensation reaction via a crosslinking mechanism. These inorganic polymers are characterised by M–O–M bonds formed by the condensation of the metallic hydroxides, (M–OH). These species condense forming progressively, oligomers, polymers, a colloid and finally gel or precipitate. The final solid can be a hydroxide or a hydrated oxide.

The metal hydroxides can be formed by hydrolysis of two kinds of precursors: salts or metallic alkoxides, the latter allowing a fine control on the properties of the final gel.

The SiO_2–Ta_2O_5 mixed oxides were prepared by mixing tetraethylortosilicate (TEOS) and tantalum pentaethoxide in 100 ml methanol. The hydrolysis of the metal alkoxide was carried out in a basic environment by the addition of 10 ml ammonium hydroxyde (NH_3 30%) to the alcoholic solution.

For the preparation of homogeneous multicomponent gels, comparable hydrolysis and polycondensation rates of precursor alkoxides are required. Unfortunately, tantalum ethoxide, similar to all transition metal alkoxides, possess a hydrolysis rate which is much quicker than that of the silicon.[13] This implies that if the hydrolysis of both tantalum and silicon alkoxides are carried out at the same time a greater number of Ta–O–Ta bonds will be formed to the detriment of Si–O–Ta bonds, giving rise to a micro heterogeneous gel.

For this reason the first step in the mixed oxide synthesis was initiation of silicon alkoxide hydrolysis by dissolving TEOS in basic ethanolic solution and stirring vigorously. After ten minutes, when TEOS hydrolysis started, the tantalum ethoxide was added. At this stage two processes occur simultaneously: (i) tantalum ethoxide hydrolysis and (ii) condensation of the formed hydroxides. The beginning of the condensation process was confirmed by the increase of the opalescence in the reaction solution. This condensation can be monometallic producing Si–O–Si or Ta–O–Ta bonds or bimetallic producing an inorganic network with Si–O–Ta characteristics bonds.

As the polymerisation reaction proceeds, the viscosity of the solution increases. After one hour of continous stirring the solution was introduced in a rotatory evaporator, where gel was formed. The gel is composed of an interconnected porous matrix, which contains alcohol, unreacted precursor and water. After one hour in the evaporator all the liquids of the mixed oxide porous structure were eliminated.

All the hydrolysis and condensation processes were carried out at room temperature. The final alkoxide molecular concentration ($Si(OEt)_4+Ta(OEt)_5$) was 0.09 M (1 M=1 mol dm^{-3}).

Table 1 presents the nomenclature of the synthesised samples with the corresponding (Ta/Ta+Si) atomic ratio.

Characterisation. A Siemens D5000 powder diffraction unit was used to obtain X-ray diffraction spectra. The powders were deposited on a silica monocrystal holder and the samples were scanned at 0.5° per min over a diffraction angle range of 1.5 to 70°. Peaks were identified by comparison with standard diffraction data.[14]

Transmission electron microscopy (TEM) of samples were

Table 1. Characteristics of Silica–Tantalum Mixed Oxides

Sample	Ta_2O_5	S_{BET}	C	Pore Volume/$cm^3\,g^{-1}$		Pore Diameter
	mol%	$m^2\,g^{-1}$		V_t	$V_{micr.}$	Å
SiTa0	0	106	126	0.55	0.01	—
SiTa5	5	442	136	0.47	0.44	42
SiTa10	10	449	120	0.33	0.20	30
SiTa20	20	353	201	0.14	0.13	27
SiTa100	100	56	215	0.04	0.00	32

carried out using a JEOL TEM SCAN X (-100) instrument, coupled with an energy dispersion spectrometer Kevex 5100. The electron acceleration tension was 100 kV.

The differential thermal analysis (DTA) and the thermogravimetric analysis (TGA) were made possible using a SETARAM TGA 92 apparatus with a heating program rate of 10 °C min^{-1} in a 120—1000 °C temperature range. Before analysis samples were dried at 120 °C for 2 h.

After degassing at 393 K for 4 h to a final pressure of 1 mmHg (1 mmHg=133.322 Pa), the silicon–tantalum mixed oxides calcined at 500 °C were characterised by N_2 adsorption/desorption isotherms[15,16] in a Micromeritics ASAP 2000 apparatus. In this way the BET surface area was calculated in the range of 0.05 to 0.2 of partial pressure. In addition to pore volume, the pore size distribution was determined by the BJH desorption branch[17] and microporous volume was calculated using the *t*-plot method.

FTIR spectra were recorded using a Brucker FT 88 spectrometer. Two kinds of measurements were carried out. Firstly, samples were pressed into self supporting disks and treated under vacuum (10^{-6} Torr, 1 Torr=133.322 Pa) at 675 K for 4 h. The spectra were recorded at room temperature. In the second method the mixed oxides were diluted in KBr to a 10% oxide/(oxide+KBr) content and spectra recorded directly.

The XPS studies were performed at room temperature on a SSX-100 "206 Surface Science Intruments (SSI)" equipment. The X-ray source was a Al anode (1486.6 eV), supplied by a monocromater. The energy scale of the spectrometer was calibrated with the Au $f_{7/2}$ binding energy fixed at 84.0 eV. The charge correction was made possible by fixing the binding energy of C 1s peak at 284.8 eV. The atomic concentration ratios were calculated by correcting the intensities, the integral of each peak, with the sensivity factors.

Results

X-Ray Diffraction. After calcination at 500 °C all samples exhibit amorphous structures, no diffraction peaks can be observed for the different XRD spectra. Calcination of SiTa100 at 900 °C, Fig. 1, produces a highly crystalline material. The obtained spectra is characteristic of the orthorhombic phase of tantalum oxide, Ta_2O_5. The crystallisation temperature for Ta_2O_5 have been previously described at 750 °C.[18] Calcination of SiTa0, SiTa5, SiTa10 and SiTa20 at 750 °C produces materials exhibiting a broad XRD spectra corresponding primarily to an amorphous silica. These mixed oxides continue to be amorphous 150 °C above the tantalum oxide crystallisation temperature, Fig. 1.

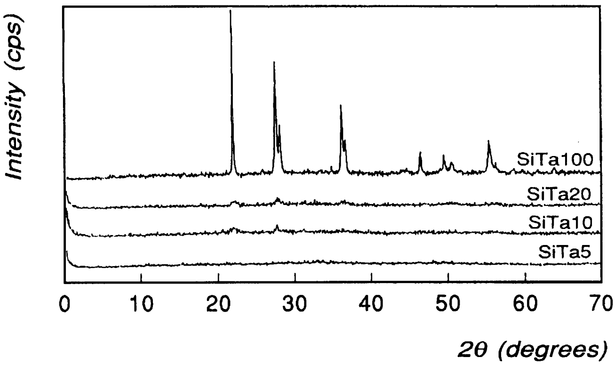

Fig. 1. X-Ray diffraction spectra, between 1.5 and 70 2θ, from SiO_2–Ta_2O_5, after thermal treatment at 900 °C.

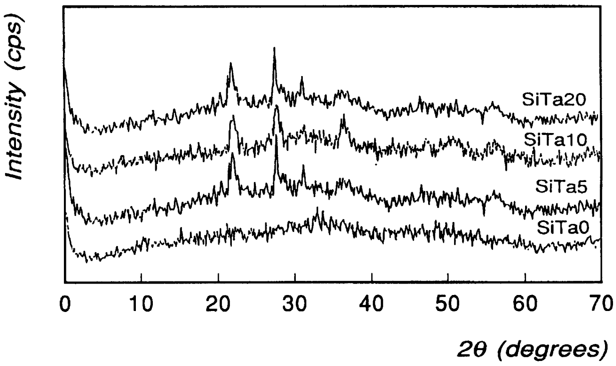

Fig. 2. X-Ray diffraction spectra of silica and SiO_2–Ta_2O_5 mixed oxides, after 1200 °C thermal treatment.

At 1200 °C, Fig. 2, the pure silica is still an amorphous. However, at this temperature the mixed oxides present three small diffraction peaks which coincide with the strongest diffraction peaks of the orthorhombic Ta_2O_5 phase.

Thermal Analysis. Figure 3, shows thermogravimetric analysis, TGA and TGD curves, for different prepared samples. The latter allows us to determined more accurately the temperature for which the weight loss is produced.

The weight loss observed during the drying procedure is mainly due to evaporation of water and organic solvent (methanol) which fill the pores of the material.

All samples presents a weight loss between 120 and 500 °C mainly due to the elimination of the residual carbon containing species. Pure silica looses almost 3% of its initial weight. SiTa100 exhibits an additional weight loss between 500 and 700 °C. This is probably due to the loss of carbon associated with the gel.[19] In fact the colour of the SiTa100 sample changed from whitish to slightly brown after treatment at 250 °C. Between 300 and 500 °C the solid turned black indicating than some carbonisation had occurred. After calcination at 700 °C the solid was again white. Tantalum oxide losses near a 10% of its initial weight.

The mixed oxides lost between 4—6% of the initial

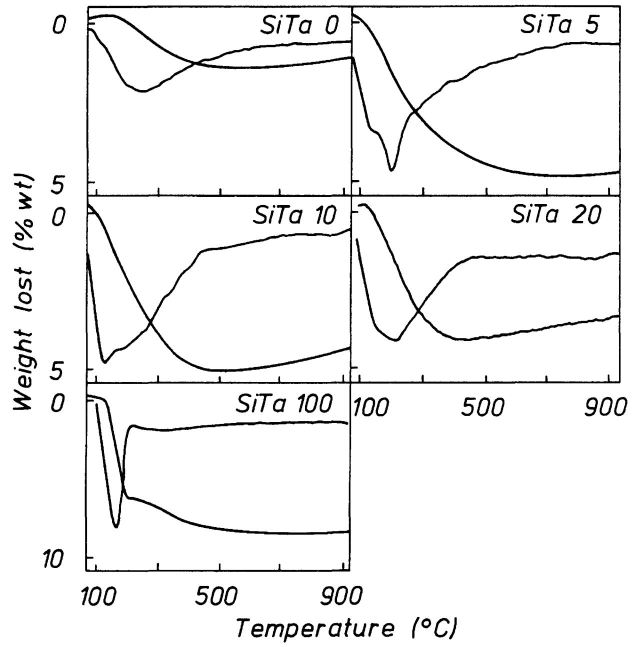

Fig. 3. TGA and TGD curved for differents oxides.

weight between 120 and 500 °C. No additional weight loss was observed above this temperature. The DTA curve indicated that the maximum weight loss is produced between 220 and 270 °C.

The differential thermal analysis, DTA of silica and silicon–tantalum mixed oxides do not exhibit nor endothermic nor exothermic peaks in the range of 120 to 1000 °C. However, the DTA curve of SiTa100, tantalum oxide presents a sharp exothermic peak near 750 °C, with no observed simultaneous weight loss.

TEM Analyses. TEM analyses were carried out on SiTa5, SiTa10, and SiTa20 samples to determined the homogeneity of the tantalum and silicon distribution in the bulk mixed oxides. A group of fifteen particles were analysed for each sample, Fig. 4.

This study shows that all the particles possess simultaneously both element: tantalum and silicon. Only in the case of SiTa10 did one particles exhibit a very low silica content.

Therefore, the most important result is than even in samples containing a 5% tantalum all the analysed particles are mixed. No pure silica was detected.

Textural Characteristics. Some of the textural characteristics of the mixed oxides determined by N_2 adsorption/desorption isotherms are presented in Table 1. The adsorption isotherm for SiTa0 is of Type IV according to the BDDT classification.[17] This isotherm type is typical of mesoporous materials. The *t*-plot curve confirms the lack of microporosity and the BJH distribution shows only pores of diameters greater than 200 Å.

Pure tantalum oxide, SiTa100, and the mixed oxides resulted similar shaped isotherms. However, the surface are a (S_{BET}) and the microporous volume increased for

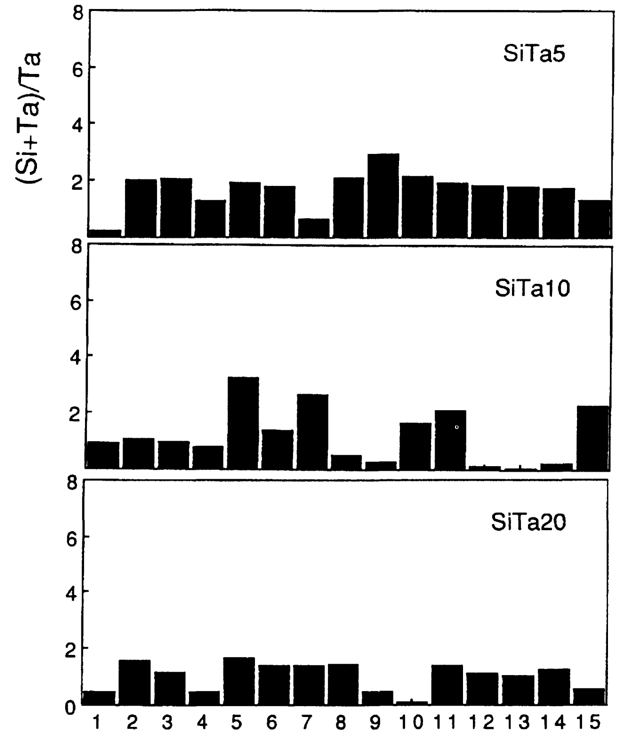

Fig. 4. TEM microanalyses for differents particles (from 1 to 15), for the mixed oxides.

mixed oxides compared to pure tantalum oxide. The surface area is four to five times greater for the mixed oxides.

In the case of SiTa5, SiTa10, and SiTa20 the N_2 adsorption/desorption isotherms show a mixed nature. At low relative pressures a large uptake of N_2 is observed which is characteristic of microporous materials. At the same time a weak hysteresis loop of Type A, which is characteristic of cylindrical mesoporous, is noted.

The mesopore size BJH distribution is unimodal and almost symmetric. The average diameter decreases with increase in tantalum content. Pore diameters greater than 40 Å were not observed in any case. This is in good agreement with the shape of N_2 isotherms and *t*-plot curves, both presenting a plateau for the adsorbed N_2 volume at $P/P_0 > 0.45$.

Since the slight difference between the up limit of microporous (20 Å) and the diameter of mesoporous in pure tantalum and mixed silice–tantalum oxides, it is not possible in *t*-plot curves to unambigously distinguish between the end of the microporous filling and the start of the capillary condensation in mesoporous. For this reason in microporous volume, Table 1, the contribution of the micro and mesopores is included. That's main porous of diameter ≥ 42 Å in the SiTa5 sample, ≥ 30 Å for SiTa10 and finally ≥ 27 Å for SiTa20.

Infrared Studies. I.R. Spectra in the Skeletal Vibration Range, KBr Pressed Disks. The FTIR spectra in the skeletal vibration range are shown in Fig. 5. The IR spectrum of SiTa0 is similar to the

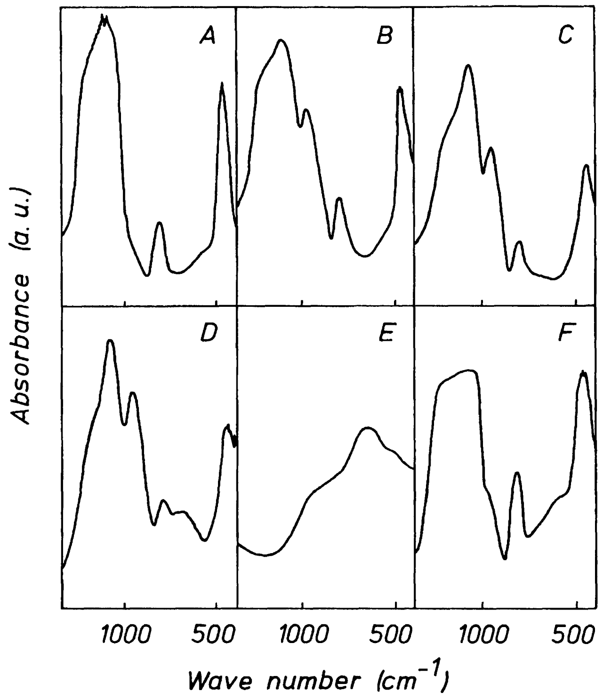

Fig. 5. FTIR spectra of A) SiTa0, B) SiTa5, C) SiTa10, D) SiTa20, and E) SiTa100, F) Mechanical mixture (KBr pressed disks).

other amorphous silica samples.[20] Three main absorption bands are observed. The strongest band corresponding to asymmetric Si–O–Si stretching, is observed at 1093 cm^{-1} along with a well resolved shoulder at 1215 cm^{-1} and another almost unresolved at 935 cm^{-1}. The symmetric Si–O–Si stretching mode is observed at 811 cm^{-1} while the deformation mode is detected at 467 cm^{-1} with a shoulder near 566 cm^{-1}.

The SiTa100 spectra shows the typical absorption bands of tantalum oxide.[21,22] This spectrum consist of three broad band below 900 cm^{-1}, a main band at 644 cm^{-1} with two well resolved shoulders at 525 and 891 cm^{-1} corresponding to the stretching modes of Ta–O bond.

The spectrum of SiTa5 is very similar to that of SiTa0 except for a well defined maximum at 960 cm^{-1}. Subtraction of the SiTa5 spectrum from that of SiTa0 shows that the addition of 5% tantalum results in the appearance of this new band. The spectra of SiTa10 and SiTa20 also present an individual maximum at 959 and 953 cm^{-1} respectively. This adsorption band near 960 cm^{-1} is not observed for pure silica, pure tantalum or in the mechanical mixtures of these two oxides. This band has already been observed in the IR spectra of SiO_2–TiO_2 and SiO_2–V_2O_5 glasses and in the spectra of crystalline titanium silicalite. Thus this adsorption band has been assigned to Si–O–Me asymmetric stretching. The wavenumber at which the maximum of this new band appears decreases with increase in tantalum content. This indicates the decrease in bond interaction strength with increase in tantalum content.

The ratio between the intensity of 960 cm^{-1} band and the 1200 cm^{-1} band (I 960 cm^{-1}/I 1200 cm^{-1}), the last one characteristic from the silica, increase with mixed oxide tantalum content.

In the SiTa20 spectra in addition to the described characteristic adsorption, a broad band with a maximum near 654 cm^{-1} is observed. This band is characteristic of the main adsorption band of tantalum oxide.

I.R. Spectra of Self Supported Disks. The samples containing silica present a cut-off at low frequencies due to skeletal vibration adsorption. The band detection limit is near 1300 cm^{-1}, Fig. 6.

In the region between 2000 and 1500 cm^{-1}, pure silica exhibits a well resolved absorption triplet due to overtone and combination modes of the skeletal vibration.[20] These bands are still observable but much more weaker in the case of SiTa5. The addition of 5% tantalum to silica greatly decreases the signal of bulk silica. In the sample containing 20% tantalum a weak signal due to bulk silica is still observed.

Examination of the adsorption bands in the 4000—3000 cm^{-1} region of self suported disks, yielded information on surface hydroxyl groups, Fig. 7.

Two adsorption bands are observed for SiTa0 in this region.[23] The first, a very sharp and symmetric band at 3750 cm^{-1}, is assigned to free OH groups on the silica surface which can be simple or geminal. The second

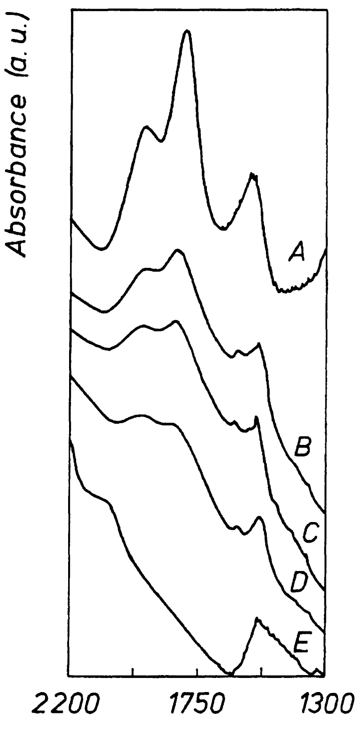

Fig. 6. FTIR spectra of selfsuported samples evacuated at 400 °C under 10^{-6} torr vacuum, A) SiTa0, B) SiTa5, C) SiTa10, D) SiTa20, and E) SiTa100.

band at lower absorption frequencies, between 3700 and 3000 cm^{-1}, is much larger and non-symmetric. This absorption is assigned to H-bonded hydroxyl groups on the surface.

The spectra, in the ν(OH) region, for samples containing both silicon and tantalum are quite similar to that of the silica alone. However, the intensity of the 3750 cm^{-1} band is slightly less and simultaneouly an important increase in the number of hydroxyl groups in the 3700—3300 cm^{-1} range is noted.

XPS. The Fig. 8 presents the surface atom ratio (Ta/Si) measured by XPS, versus the theoretic bulk composition. This figure shows that the atomic ratio obtained for the solid surface is in good agreement with theoretic values obtained for the bulk solid.

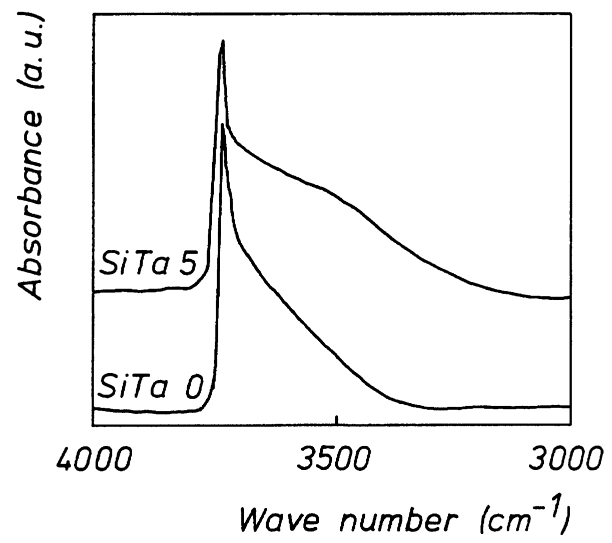

Fig. 7. FTIR spectra in hydroxyl group region of the pure powder samples evacuated at 400 °C under 10^{-6} Torr vacuum.

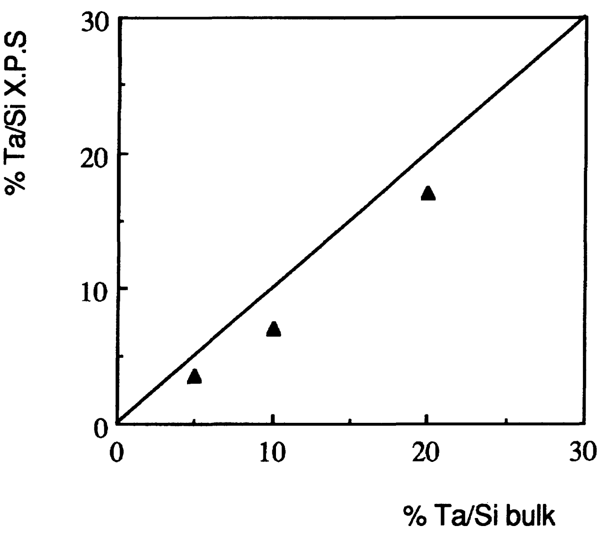

Fig. 8. Ta/Si atom percentage measured by XPS, (Si2p and Ta4$d_{5/2}$ lignes), varsus expected bulk composition.

Table 2. Core Electron Binding Energies (eV) for SiO_2–Ta_2O_5 Mixed Oxides

Sample	O1s		Si2p	Ta4$d_{5/2}$
SiTa0	532.8	—	103.7	—
SiTa5	532.8	531.0	103.5	231.6
SiTa10	532.8	531.0	103.5	231.3
SiTa20	532.7	531.0	103.2	231.2
SiTa100	532.3	530.8	—	230.2

Table 2 shows the core lines, measured by XPS, for the different SiO_2–Ta_2O_5 mixed oxides. The binding energy of the Si2p line decreases with decrease in the level of silicon in the mixed oxide samples. The 103.7 eV value observed for SiTa0 is typical of silica gels, and the Si2p energy can decrease to much lower values i.e. 102 eV, as the case of silicalites. Similarly concerning the Ta4$d_{5/2}$ line, a greater binding energy is observed for SiTa20 compared to pure Ta_2O_5[24)] and this binding energy increases with decrese in tantalum content. The increase in binding energy from Ta_2O_5 to the mixed oxide containing a 5% Ta_2O_5 correspond to 1.8 eV.

In pure tantalum oxide the O1s band is asymmetric, it can be deconvolued into two 85% Gaussien components. This asymmetry is explained by the different electric density of two kinds of oxygen existing in tantalum oxide. First the oxygen influenced by hydroxyl groups on the surface, presenting a minor component near 352.3 eV and second the oxygen in bulk tantalum oxide producing the main component near 530.8 eV.[24)]

Discussion

Upon thermal treatment, the behavior of tantalum oxide in the SiO_2–Ta_2O_5 mixed oxide's matrix is quite different from that of pure tantalum oxide.

Pure tantalum oxide presents diffraction peaks typical of the crystalline orthorhombic Ta_2O_5 phase after thermal treatment at 700 °C. This is confirmed by DTA which exhibits an exothermic peak near 760 °C, representing the temperature at which tantalum oxide crystallizes. For SiO_2–Ta_2O_5 mixed oxide no such crystalline diffraction peaks can be observed after calcination at 700 °C. A much severer calcination treatment, of approximately 1200 °C, is required before the first sign of crystallization. The DTA curves between 120 and 1000 °C shows no evidence of crystallisation.

This difficulty associated with the crystallisation process have been previously observed for different cases of mixed oxides prepared by the sol–gel method i.e., SiO_2–Nb_2O_5,[6)] TiO_2–ZrO_2;[9)] V_2O_5–TiO_2, V_2O_5–TiO_2–SiO_2,[25)] and SiC/TaC.[26)] Even for tantalum modified polycarboxylates[26)] crystallization is not observed below 1400 °C.

The mixed oxide, SiTa20, contains a high level of tantalum (Ta/Ta+Si=16 at %). Thus it can be concluded that if pure tantalum oxide existed in the mixed oxide matrix characteristic diffraction peaks would be observed. However, the tantalum oxide aggregate dispersion was so that it was not observed by X-ray diffraction.

The existence of an intimate mixture, at a molecular level, in mixed oxides synthesised by the sol–gel method, has been already claimed in many publications.$^{27)}$ This phenomenon could be the source of the difficulty of tantalum oxide crystallisation at low temperatures. The interaction at the molecular level between the silica and the tantalum oxide would retard the solid state diffusion. Therefore changes in the solid matrix due to thermal treatment would be limited.

The relationship between the Ta/Si atomic ratio, at the solid surface, calculated by XPS, and the Ta/Si ratio expected in the bulk solid for the different SiO_2–Ta_2O_5 mixed oxides is shown in Fig. 8. The values for the surface and bulk composition are in good agreement. This confirms the homogeneous distribution of the silicon and tantalum in the bulk solid.

The microanalyses carried out by TEM further support the idea of the existence of an intimate mixture of elements: silicon and tantalum in the mixed oxide matrix. Particles formed exclusively by tantalum oxide or silica were not detected. Even in a sample containing only 5 atomic % tantalum, pure silica particles were not detected. This is certainly due to the effective incorporation of tantalum in silica network.

However the microanalyses show the inhomogeneous distribution of the tantalum content in different particles of the same sample. Therefore, even if all particles possess a mixed composition (SiO_2–Ta_2O_5) the tantalum and silicon content for all particles of the same sample is not identically the same. This phenomenon of inhomogeneity has been already reported in the literature, it is inherent to the synthesis method and limited to the particle level.$^{28)}$

Studies carried out by nitrogen adsorption/desorption isotherms show that the introduction of tantalum in the silica network changes the formed xerogel texture.

The BET surface area of the mixed oxides is much larger than those of the pure silicon or tantalum oxides. For mixed oxides with a 5 or 10 atomic % tantalum, the surface area is between 4 and 5 times bigger than the silica alone. The increase of the tantalum content up to 10% results in a decrease of the developed surface area. The increase of surface area in the mixed oxides is due to the formation of a porous structure. This is basically mesopores, of 30 to 40 Å, with a very narrow unimodal pore size distribution.

The textural characteristics of the SiTa0, including mesopores of sizes up to 200 Å, a surface area of 120 $m^2 g^{-1}$ and a IV type N_2 adsorption/desorption isotherm, is typical of a silica formed in a basic catalysed sol–gel process.$^{24)}$ Under basic conditions network forming is favored in the gelation process. The produced sol is of a cluster type and the final gel is colloidal. The contact between clusters formed in the colloidal gel synthesis is rigid. The capillary force in the calcination produce the break down of the structure and the final solid specific surface is small.

On the other hand, the 5, 10, and 20 per cent Ta/(Ta+Si) mixed oxides show a porous structure completely different from the SiTa0. Their textural characteristics are typical of materials which result from the calcination of polymeric gels. This kind of gel is formed by slightly inter-bonded polymeric chains. The addition of tantalum in the initial silica precursor produces a structural transformation from a colloid to a polymeric gel.$^{30)}$ This results in a different texture with a unimodal well defined pore size (30—40 Å) and a larger specific surface area.

The SiO_2–Ta_2O_5 gels are formed by a condensation reaction between the partially hydrolysed metal hydroxides, resulting in a polymeric growth of the gel via cross-linking. By analogy with this theoretic model the Ta–O–Si bond will be formed in the SiO_2–Ta_2O_5 mixed gel.

The analyses of the mixed oxides by FTIR and XPS permits the study of the chemical environment of the different atoms and yields information as to wheather a new kind of bond, not present in the pure oxides have been formed.

The FTIR measurements carried out between 1500 and 2000 cm^{-1} using selfsupported samples show a progressive decrease in the Si–O–Si triplet overtone signal when the tantalum content is increased. This signal, considered to be due to the bulk silica, is significantly reduced after a 5% addition of tantalum in the silica network. This triplet is barely visible for SiTa20. This observation confirms the rapid decrease of the bulk silica present in the mixed oxide, by the incorporation of tantalum in the silica matrix.

The most interesting aspect of the FTIR spectra of the mixed oxides is the appearance of a new band near 960 cm^{-1}. This band is not observed in the spectra of silica, tantalum oxide, or Ta_2O_5/SiO_2 mechanical mixture.

Similar observations have been already described for titanium$^{31)}$ and vanadium$^{32)}$ silicalite, and for TiO_2–SiO_2 mixed oxides and glasses.$^{33)}$ The bands near 960 cm^{-1} are characteristics of metal–oxygen stretching vibrations. Recent studies carried out by FTIR show that the same 960 cm^{-1} band appearing in titanium silicatites can be assigned to the stretching mode of the SiO_4 network bonded to Ti^{4+} atom.$^{31,33)}$ These results strongly suggest the existence of a Si–O–Ta bond in the synthesised multicomponent oxide.

A study of the chemical environment of atoms in pure and mixed oxides were carried out by XPS. The charge density effect on oxygen and cations have been studied using the binding energie values of the $Ta4d_{5/2}$, Si2p and O1s electrons. Using a simple electrostatic model it can be predicted that the binding energy for the internal orbital will increase with decrease in the electronic density of the external orbital.$^{34)}$

When the effective electronic charge upon an atom decreases the binding energy of each electron increases. Using this model, a comparative study of the O1s bending energies in the pure and mixed oxides have been carried out. The difference between the O1s binding energy in SiTa0 (O1s=532.8 eV) and SiTa100 (O1s=530.8 eV) denote a larger electronic density of oxygen in tantalum oxide than in silica. This agrees with Sanderson's electronegativity values, tantalum is more electropositive than silicon.

The changes in the silicon and tantalum electronic density are reflected by the $Ta4d_{5/2}$ and Si2p binding energies.

The decrease in the Si2p binding energy from silica gel (Si2p=103.7 eV) to SiTa20 (Si2p=103.2 eV) can be interpreted as an increase in the silicon external orbital electronic density. In the same way, the increase in the SiTa20 ($Ta4d_{5/2}$=231.3 eV) in relation to pure tantalum oxide ($Ta4d_{5/2}$=230.2 eV) can be interpreted as a decrease in the electronic density of the outter orbital of tantalum in the mixed oxides.

The decrease in Si2p binding energy coupled with the increase in the $Ta4d_{5/2}$ binding energy exhibited by the silicon–tantalum mixed oxides compared to the pure oxides, could be due to the formation of a Ta_2O_5–SiO_2 glass where the Si–O–Ta bond will be present.

Conclusions

For the first time the synthesis of Ta_2O_5–SiO_2 mixed oxides have been made possible, thanks to the sol–gel method.

The silicon tantalum mixed oxides possess a great stability to thermal aggregation as shown by the absence of the diffraction peak of tantalum oxide below 1200 °C. For pure tantalum oxide this orthorhombic crystalline phase forms at 750 °C.

No segregation between surface and bulk oxides was observed by XPS, and TEM analysis shows that a silicon tantalum mixture exist even in the mixed oxide submicrometrics particles. The existence of a intimate mixture of the tantalum and silicium elements at the molecular level can be concluded.

The studies carried out by N_2 adsorption/desorption isotherms shows that tantalum addition to silica precursor produces a large textural alteration. The surface area of the mixed oxides is up to four times larger than the original silica. The textural characteristics of the SiTa0 suggest a colloidal gel formation, the addition of tantalum in $Ta/Ta+Si \geq 5\%$ indicates the formation of a polymeric gel.

FTIR measurements carried out on selfsupported samples between 1500 and 2000 cm^{-1} showed clearly the decrease of the bulk silica signal with the incorporation of tantalum into the mixed oxides. Nevertheless the most interesting information provided by infrared measurement is the appearance, for the mixed oxides, of a new band near 960 cm^{-1}, which, from the literature information, can be associated with the Si–O–Ta bond.

The XPS results analysed by a simple electrostatic model seems to support of the existence of a Si–O–Ta interaction.

These silicon–tantalum mixed oxides, which can be described as amorphous inorganic covalent materials, constitute a new non crystalline solid family.

We wish to thank "Eusko Jaurlaritza" (Grant BFI90.061. Modalidad AK) and the "Service de la Programmation de la Politique Scientique, Belgium" for the financial support. We express our thanks Dr. T. Curtin for reviewing the manuscript.

References

1) P. Coussin and R. A. Ross, *Mater. Sci. Eng.*, **A130**, 119 (1990).
2) M. A. Cauqui and J. M. Rodríguez-Izquierdo, *J. Non-Cryst. Solids*, **147**, 724 (1992).
3) K. Tanabe, T. Sumiyoshi, K. Shibata, T. Kiyoura, and J. Kitagawa, *Bull. Chem. Soc. Jpn.*, **47**, 1064 (1974).
4) K. Shibata, T. Kiyoura, J. Kitawa, T. Sumiyoshi, and K. Tanabe, *Bull. Chem. Soc. Jpn.*, **46**, 2985 (1973).
5) T. Lopez, *React. Kinet. Catal. Lett.*, **47**, 21 (1992).
6) P. A. Burke and E. I. Ko, *J. Catal.*, **129**, 38 (1991).
7) A. Baiker, P. Dollenmeier, M. Glinski, A. Reller, and V. K. Sharma, *J. Catal.*, **111**, 273 (1988).
8) A. Thangaraj, R. Kumar, S. P. Mirajkar, and P. Ratnasamy, *J. Catal.*, **130**, 1 (1991).
9) J. G. Weissman, E. I. Ko, and S. Kaytal, *Appl. Catal. A: General*, **94**, 45 (1993).
10) G. M. Pajonk, *Appl. Catal.*, **72**, 217 (1991).
11) C. W. Turner, *Ceram. Bull.*, **70**, 1487 (1991).
12) C. J. Brinker and G. W. Scherer, "Sol–Gel Science. The Phisics and Chemistry of Sol–Gel Processing," Academic Press, New York (1990).
13) J. Livage, M. Henry, and C. Sanchez, *Prog. Solid State Chem.*, **18**, 259 (1988).
14) J. Harvey and H. Wilman, *Acta Crystallogr.*, **14**, 1278 (1961).
15) S. J. Gregg and K. S. W. Sing, "Adsorption, Surface Area and Porosity," Academic Press, London (1982).
16) J. Seifert and G. Emig, *Int. Chem. Eng.*, **31**, 29 (1991).
17) S. Lowell and J. E. Shields, "Powder Surface Area and Porosity," ed by B. Scarlett, "Powder Technology Series," Chapman and Hall, London and New York (1988).
18) T. Ushikubo and K. Wada, *Appl. Catal.*, **67**, 25 (1990).
19) H. C. Ling, M. F. Ynag, and W. W. Rhodes, "Science of Ceramic Chemical Processing," ed by L. L. Hech and D. R. Ulrich, Wiley-Interscience Publication, New York (1986), p. 285.
20) J. Y. Ying and J. B. Benziger, *J. Non-Cryst. Solids.*, **147**, 222 (1992).
21) P. Phulé, *J. Mater. Res.*, **8**, 334 (1993).
22) U. Balachandran and N. G. Eror, *J. Mater. Sci. Lett.*, **1**, 219 (1982).
23) H. P. Böhm and H. Knözinguer, "Catalysis-Science and Technology," ed by J. R. Andersen and M. Boudart,

(1984), Vol. 4.

24) F. Garbassi, J. C. J. Bart, and G. Petrini, *J. Electron Spectros.*, **22**, 95 (1981).

25) B. E. Handy, M. Maciejewski, and A. Baiker, *J. Catal.*, **134**, 75 (1992).

26) K. Thorne, E. Limatta, and J. D. Mackenzie, *J. Mater. Res.*, **6**, 2199 (1991).

27) A. Wokaun and M. Schraml, *J. Catal.*, **116**, 595 (1989).

28) A. B. Hardy, W. E. Rhine, and H. K. Bowen, *J. Am. Ceram. Soc.*, **76**, 97 (1993).

29) B. Handy, K. L. Walther, A. Wokaum, and A. Baiker, "Scientific Bases for the Preparation of Heterogeneous Catalysts," in "5th International Symposium," 1990.

30) J. Livage, M. Henry, and J. P. Jolivet, "Multifunctional Mesoporous Inorganic Solids," ed by C. A. C. Sequeira and M. J. Hudson, Kluer Academic Publishers, Netherlands (1993), p. 321.

31) J. A. Martens, Ph. Buskens, P. A. Jacobs, A. van der Pol, J. H. C. van Hooff, C. Ferrini, H. W. Kouwenhoven, P. J. Kooyman, and H. van Bekkum, *Appl. Catal. A: General*, **99**, 71 (1993).

32) P. R. Hari Prasad Rao, A. V. Ramaswamy, and P. Ratnasamy, *J. Catal.*, **137**, 225 (1992).

33) C. U. I. Odenbrand, S. L. T. Andersson, L. A. H. Andersson, J. G. M. Brandin, and G. Busca, *J. Catal.*, **125**, 541 (1990).

34) H. Holler, J. A. Lercher, and H. Vinek, *Mater. Chem. Phys.*, **18**, 577 (1988).